Subunit Interactions in the Activation of Cyclic Nucleotide-Gated Ion Channels

Michael D. Varnum and William N. Zagotta
Department of Physiology and Biophysics, Howard Hughes Medical Institute, University of Washington, Seattle, Washington 98195 USA

ABSTRACT Cyclic nucleotide-gated (CNG) ion channels of retinal photoreceptors and olfactory neurons are multimeric proteins of unknown stoichiometry. To investigate the subunit interactions that occur during CNG channel activation, we have used tandem cDNA constructs of the rod CNG channel to generate heteromultimeric channels composed of wild-type and mutant subunits. We introduced point mutations that affect channel activation: 1) D604M, which alters the relative ability of agonists to promote the allosteric conformational change(s) associated with channel opening, and 2) T560A, which primarily affects the initial binding affinity for cGMP, and to a lesser extent, the allosteric transition. At saturating concentrations of agonist, heteromultimeric channels were intermediate between wild-type and mutant homomultimers in agonist efficacy and apparent affinity for cGMP, cIMP, and cAMP, consistent with a model for the allosteric transition involving a concerted conformational change in all of the channel subunits. Results were also consistent with a model involving independent transitions in two or three, but not one or four, of the channel subunits. The behavior of the heterodimers implies that the channel stoichiometry is some multiple of 2 and is consistent with a tetrameric quaternary structure for the functional channel complex. Steady-state dose-response relations for homomultimeric and heteromultimeric channels were well fit by a Monod, Wyman, and Changeux model with a concerted allosteric opening transition stabilized by binding of agonist.

INTRODUCTION

Cyclic nucleotide-gated (CNG) channels are important in the signaling pathway for communication of sensory information in retinal photoreceptors (Yau and Baylor, 1989) and olfactory receptor neurons (Lancet, 1986; Zufall et al., 1994), where they respond to changes in intracellular concentrations of cGMP and cAMP, respectively. CNG channels have also been identified in other tissue types, such as heart (Biel et al., 1994), pineal gland (Dryer and Henderson, 1991; Distler et al., 1994), kidney (Biel et al., 1994), and sperm (Biel et al., 1994; Weyand et al., 1994), where their functional roles are less well defined. Whereas CNG channels can be heterologously expressed in *Xenopus* oocytes or in HEK 293 cells as multimers of identical subunits, coexpression of recently identified second subunits confers channel properties that more closely resemble those of native preparations from photoreceptors (Chen et al., 1993; Korschen et al., 1995) or olfactory receptor neurons (Bradley et al., 1994; Liman and Buck, 1994).

Two of the central questions for ion channel function are: What is the nature of the conformational changes that occur during channel activation, and How do the individual subunits of a multi-subunit channel interact? These questions are not unique to ion channels, being applicable to other enzymes composed of multiple identical or homologous subunits. Several specific features of CNG channels make them well suited for investigating protein conformational changes in general. First, ion channel proteins can be studied by using powerful patch-clamp techniques. Second, cyclic nucleotide-gated channels are part of a functionally diverse family of proteins that share a homologous nucleotide-binding domain and are activated or regulated by cyclic nucleotide binding; these include plant inward-rectifier channels (KAT1, AKT1), *eag*-like channels, cAMP- and cGMP-dependent protein kinases, and the catabolite gene activator protein of *Escherichia coli* (CAP) (Shabb and Corbin, 1992). The structure of the ligand-binding domain of CAP and the regulatory subunit of cAMP-dependent protein kinase have been determined by x-ray crystallography (Weber and Steitz, 1987; Su et al., 1995). These structures provide a good starting point for understanding the structure and function of CNG channel proteins. Third, a specific molecular interaction has been recently identified that is integral to translating ligand binding to the conformational changes associated with channel opening. Mutation of a single amino acid in the putative C α helix of the cyclic nucleotide-binding domain of the rod CNG channel (aspartic acid 604) can invert agonist selectivity, converting a channel that is highly selective for cGMP to one that prefers cAMP (Varnum et al., 1995). This resulted from an alteration in the relative efficacy of the agonists rather than a change in initial binding affinity. Naturally occurring amino acid differences at this position in the cyclic nucleotide-binding domain can account for the different agonist selectivities of CNG channels (e.g., the fish olfactory channel—see Goulding et al., 1992, 1994; and the rat olfactory channel—see Dhallan et al., 1990) and for the increased sensitivity to cAMP conferred by coexpression of the rat olfactory subunit 2 with subunit 1 (Bradley et al., 1994; Liman and Buck, 1994).

Received for publication 29 November 1995 and in final form 16 February 1996.

Address reprint requests to Dr. William N. Zagotta, Department of Physiology and Biophysics, Howard Hughes Medical Institute, Box 357370, University of Washington, Seattle, WA 98195. Tel.: 206-685-3878; Fax: 206-543-0934; E-mail: zagotta@u.washington.edu.

0006-3495/96/06/2667/13 $2.00

In this study we have used tandem cDNA constructs to control the stoichiometry of mutant and wild-type channel subunits in heteromultimeric channels, in order to examine subunit interactions during CNG channel gating. This has been a fruitful strategy for voltage-dependent potassium channels for understanding the mechanisms of binding of pore blockers (Heginbotham and MacKinnon, 1992; Kavanaugh et al., 1992; Liman et al., 1992; Hurst et al., 1992), voltage-dependent activation (Tytgat and Hess, 1992; Hurst et al., 1992; McCormack et al., 1992), and inactivation (Ogielska et al., 1995). Although the subunit stoichiometry of CNG channels is unknown, the sequence similarity with potassium channels suggests that their functional composition may be a tetramer (Jan and Jan, 1990; Kaupp and Koch, 1992; MacKinnon, 1991; Shen et al., 1994). If CNG channels contain four homologous subunits, then expression of heterodimers composed of mutant and wild-type subunits would specify that the mutations would be present in two of the four subunits. We will analyze the effect of specific mutations in these heteromultimeric channels on CNG channel gating. In the first part of the paper, we focus on events occurring after cyclic nucleotide binding by looking at saturating cyclic nucleotide concentrations. In the second part, we consider a specific model for CNG channel activation that includes cyclic nucleotide binding.

MATERIALS AND METHODS

Molecular biology

Site-specific mutations were generated by oligonucleotide-directed mutagenesis using polymerase chain reaction to generate cassettes containing the desired mutation. These were subcloned to replace the corresponding region of the wild-type bovine rod channel (Kaupp et al., 1989) and confirmed by sequencing, as previously described (Gordon and Zagotta, 1995a). Tandem cDNA constructs were generated by replacing the stop codon of one subunit (the A protomer) with DNA encoding a short linker sequence (Q_8IEGRQ_8A) followed by an *Nco*I site. For the second subunit (the B protomer) an *Nco*I site was introduced at the start codon, creating a K2E mutation. Protomers were linked, using these *Nco*I sites and another unique restriction site outside the coding region, and subsequently checked for recombination on ethidium bromide-stained agarose gels. For experiments examining the effects of T560A mutation, the amino acid sequence of wild-type and mutant subunits differed from the published sequence (Kaupp et al., 1989) containing an alanine-to-valine substitution at position 483; this caused a small decrease in the apparent affinity for cGMP (data not shown). Oocyte preparation and cRNA transcription and expression were carried out as previously described (Zagotta et al., 1989).

Electrophysiology

Patch-clamp experiments were performed with an Axopatch 200A amplifier (Axon Instruments, Foster City, CA) in the inside-out configuration. Currents were low-pass filtered at 2 kHz (8-pole Bessel) and sampled at 10 kHz. Recordings were made at 20–22°C. Data were acquired and analyzed using a Macintosh computer and Pulse software (Instrutech, Elmont, NY). Initial pipette resistances were 0.5–1 MΩ. Intracellular and extracellular solutions contained 130 mM NaCl, 0.2 mM EDTA, and 3 mM HEPES (pH 7.2). The pipette solution also included 500 μM niflumic acid to reduce endogenous calcium-activated chloride currents; niflumic acid had no effect on cyclic nucleotide-activated currents (data not shown). Intracellular solutions containing cyclic nucleotides were changed using an RSC-100 rapid solution changer (Molecular Kinetics, Pullman, WA). Currents in the absence of cyclic nucleotide were subtracted.

We estimated the fraction of the channels activated (I/I_{max}) by comparing the macroscopic current to the maximum current obtained after potentiation by Ni^{2+} (Gordon and Zagotta, 1995a) at saturating concentration of the best agonist. For Ni^{2+} potentiation, EDTA in the intracellular solution was replaced by 1 μM or 10 μM $NiCl_2$. In the presence of 10 μM Ni^{2+} (for T560A dimers), block of current was estimated to be 10 ± 7%, from the effect on nonpotentiating H420Q channels and rapid solution changes in wild-type channels (Gordon and Zagotta, 1995a). Therefore, determinations of I/I_{max} for T560A experiments were corrected for this block. Block of current by 1 μM Ni^{2+} was negligible (data not shown).

Theory

We examined two general classes of schemes to describe how the conformational changes associated with CNG channel activation may occur: 1) the allosteric transitions after ligand binding involve independent conformational changes in one or more of the channel subunits (independent models; Fig. 2 *A*), and 2) the allosteric transition(s) involve cooperative interactions between subunits, the extreme representative of this being a single concerted allosteric transition involving all of the subunits (cooperative model; Fig. 2 *B*). For the independent models, we predicted the apparent equilibrium constant (L_{app}) of the allosteric transition(s) for heteromultimeric channels composed of two mutant and two wild-type subunits, treating the ensemble of fully liganded closed and open states as a single closed-to-open transition. For a model involving independent transitions in all four subunits of a heterotetrameric channel,

$$L_{app} = \frac{l^2m^2}{1 + 2l + 2m + l^2 + m^2 + 4lm + 2l^2m + 2lm^2}, \quad (1)$$

where l and m are equal to the equilibrium constants for the individual transitions for wild-type and mutant subunits, respectively. For homomultimeric channels, $l = m$ in the equation above. l and m were calculated for each model from the behavior of the respective homomultimeric channels. For a model where independent transitions in three subunits of a heterotetrameric channel are sufficient for channel activation,

$$L_{app} = \frac{l^2m^2 + 2l^2m + 2lm^2}{1 + 2l + 2m + l^2 + m^2 + 4lm}. \quad (2)$$

For a scheme in which independent transitions in any two subunits of a heterotetrameric channel are sufficient for activation,

$$L_{app} = \frac{l^2m^2 + 2l^2m + 2lm^2 + l^2 + m^2 + 4lm}{1 + 2l + 2m}. \quad (3)$$

For a model where an independent transition in one of the subunits of a heterotetrameric channel is sufficient for channel opening,

$$L_{app} = l^2m^2 + 2l^2m + 2lm^2 + l^2 + m^2 + 4lm + 2l + 2m. \quad (4)$$

From the aggregate equilibrium constant L_{app}, we calculated the apparent change in free energy for the allosteric transition(s) ($\Delta G_{L_{app}}$), and the $\Delta G_{L_{app}}$ predicted by each of the models, using the following equation:

$$\Delta G_{L_{app}} = -RT \ln (L_{app}). \quad (5)$$

For the concerted model (Fig. 2 *B*), we predicted the free energy change for the allosteric transition of the heteromultimeric channels using the following equation:

$$\Delta G_L = \frac{\Delta G_L^{wt} + \Delta G_L^{m}}{2}, \quad (6)$$

where ΔG_L^{wt} and ΔG_L^m are the free energy differences for the allosteric transition of wild-type and mutant homomultimeric channels, respectively.

We also considerd a specific gating scheme for cyclic nucleotide binding and channel activation that includes a concerted conformational transition to the open state, the allosteric model of Monod, Wyman, and Changeux (MWC; Scheme 1 and Fig. 8) (Monod et al., 1965). In this model, the channel exists in either of two reversibly accessible quaternary conformations: tense or closed (C) and relaxed or open (O). The allosteric transition between the closed and open conformations is promoted by binding of ligand to each of four binding sites. For heteromultimeric channels, the equilibrium constant for the allosteric transition depends on which of the subunits are occupied by ligand (Fig. 8). Fractional activation (I/I_{max}) was calculated for the MWC model using a general equation to calculate the equilibrium open probability for any model. For any model containing sequentially numbered states, the equilibrium probability of being in the open state is given by the following equation:

$$P_o = \frac{\sum_{i=\text{open states}} \left(\prod_{j=1}^{i} X_j \right)}{\sum_{i=\text{all states}} \left(\prod_{j=1}^{i} X_j \right)}, \quad (7)$$

where X_j indicates the unimolecular equilibrium constant between states $j-1$ and j, and $X_1 = 1$. If the transition between states $j-1$ and j involves the binding of ligand, then X_j = [cNMP] K_j, where K_j indicates the bimolecular equilibrium constant. The term $\Pi_{j=1}^{i} X_j$ is defined as the product of the equilibrium constants for any pathway from state 1 to state j. This equation was used for Scheme 1 for homomultimeric channels and for the scheme displayed in Fig. 8 for heteromultimeric channels.

RESULTS

To assess the practicality of using tandemly linked channel subunits for investigating CNG channel gating, we compared the functional properties of bovine rod CNG channels, as expressed from either a monomeric or concatenated cDNA construct (Fig. 1). Monomeric constructs or tandem constructs coding for two channel subunits, covalently attached by a linker region of 22 amino acids, were expressed in *Xenopus* oocytes, and electrical recordings were made in membrane patches in the inside-out configuration. In Fig. 1, current families elicited by voltage steps from 0 mV to voltages from −80 to +80 mV are shown for wild-type monomers (wt) and dimers (wt/wt), and D604M monomers (D604M) and dimers (D604M/D604M), activated by saturating cGMP (8 mM; Fig. 1 *A*) and saturating cAMP (32 mM; Fig. 1 *B*). Each macropatch represents a large population of channels. We estimated the fraction of the channels that are activated by the ratio between the macroscopic current and the maximum current obtained after Ni^{2+} potentiation at saturating concentration of the best agonist (I/I_{max}). Ni^{2+} has previously been shown to promote nearly maximum activation of rod channels at saturating concentration of cGMP by binding preferentially to the open state of the channel. The site of action for Ni^{2+} was shown to be outside the putative cyclic nucleotide binding domain (Gordon and Zagotta, 1995a). A quantitatively similar effect of Ni^{2+} on the allosteric transition was seen with different cyclic nucleotides and with mutations outside the Ni^{2+} binding site (Gordon and Zagotta, 1995b). Using the previously determined model for potentiation and binding affinity for Ni^{2+} (Gordon and Zagotta, 1995a), we have calculated the error in estimating the fractional activation with I/I_{max}. For all of the mutants examined, the greatest error predicted for this estimation of fractional activation was less than 2.5%.

For each family of traces (Fig. 1, *A* and *B*), display of the currents was scaled proportional to the maximum current obtained after Ni^{2+} potentiation (I_{max}), to facilitate comparison of agonist efficacy. The fractional activation evoked by saturating concentrations of agonist (I_{sat}/I_{max}) was similar for monomers and dimers. Furthermore, for channels expressed from either monomeric (wt and D604M) or dimeric (wt/wt and D604M/D604M) constructs, the D604M mutation similarly inverted agonist efficacy, decreasing the effectiveness of cGMP (Fig. 1 *A*) and increasing the effectiveness of cAMP (Fig. 1 *B*).

Dose-response curves for wild-type and mutant channels assembled from dimers resembled their respective counterparts expressed from monomeric constructs for activation by cGMP (Fig. 1 *C*) or cAMP (Fig. 1 *D*). Fits of dose-response curves with the Hill equation yielded a similar $K_{1/2}$, Hill coefficient, and fractional activation at saturating ligand concentrations (I_{sat}/I_{max}) for dimeric constructs compared to expression from monomeric constructs (Table 1). Tandem linkage of subunits created only a small decrease in the maximum current elicited by saturating cyclic nucleotide and a small decrease in the apparent affinity for cGMP compared to currents from expression of monomeric channel subunits. Overall, these results demonstrate that expression of tandemly linked proteins comprised of two subunits of the CNG channel does not substantially alter the macroscopic behavior of the channels, and furthermore suggests that these dimeric constructs may by useful for studying CNG channel gating.

TABLE 1 Wild-type and D604M CNG channels expressed from monomeric or dimeric cDNA constructs

	cGMP				cAMP			
	$K_{1/2}$ (μM)	Hill coeff.	I_{sat}/I_{max}	n	$K_{1/2}$ (μM)	Hill coeff.	I_{sat}/I_{max}	n
wt	58 ± 13	2.0 ± 0.2	0.950 ± 0.023	9	3061 ± 1007	1.5 ± 0.2	0.016 ± 0.006	9
wt/wt	98 ± 19	1.9 ± 0.1	0.914 ± 0.046	5	2867 ± 1856	1.4 ± 0.1	0.007 ± 0.004	5
D604M	271 ± 89	1.5 ± 0.1	0.032 ± 0.008	6	1993 ± 620	1.2 ± 0.1	0.175 ± 0.037	6
D604M/D604M	452 ± 290	1.1 ± 0.2	0.029 ± 0.017	6	1682 ± 861	1.2 ± 0.2	0.160 ± 0.075	6

Data expressed as mean ± SD.

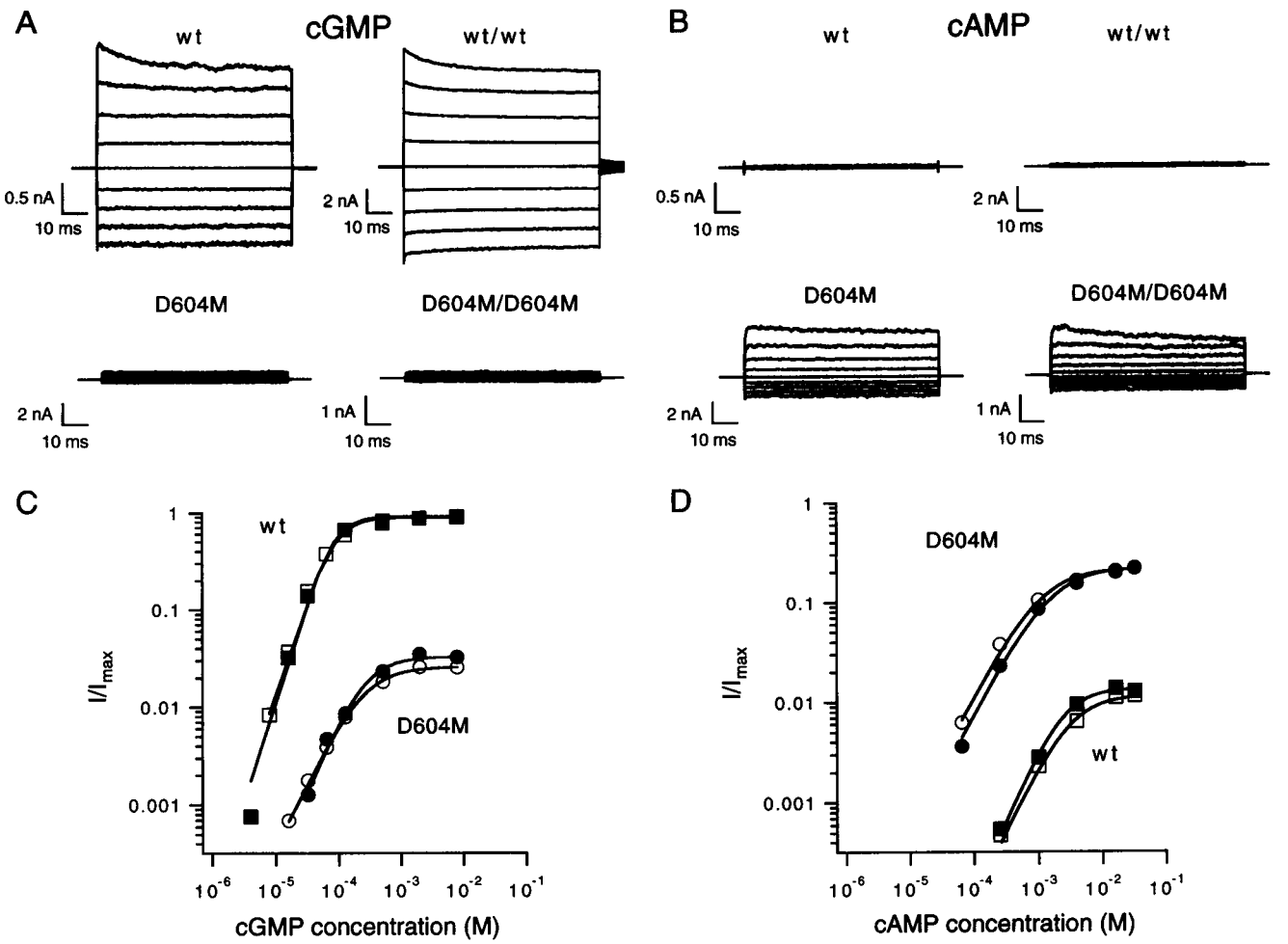

FIGURE 1 Current families are shown from inside-out patches excised from *Xenopus* oocytes expressing wild-type and mutant channels, from either monomeric or dimeric constructs. Currents were elicited by 8 mM cGMP (*A*) or 32 mM cAMP (*B*) and voltage pulses from 0 mV to potentials between −80 and +80 mV in 20 mV-steps. Control currents in the absence of cyclic nucleotide were subtracted. The currents were scaled (using the +60 mV trace) to the maximum current obtained after Ni^{2+} potentiation (Gordon and Zagotta, 1995a) at a saturating concentration of the best agonist (I_{max}). The dose-response relationship is shown for activation of wild-type and D604M channels expressed from monomeric or dimeric constructs, in response to cGMP (*C*) and cAMP (*D*). Squares indicate wild-type channel subunits and circles denote D604M mutant subunits; closed symbols denote expression from monomeric constructs and open symbols indicate expression of tandemly linked dimeric constructs. Currents were measured at +60 mV between 70 and 80 ms for small currents and within the first 5 ms for large currents, to minimize the effect of ion depletion (Zimmerman et al., 1988). The fractional activation (I/I_{max}) was estimated from Ni^{2+} potentiation (Gordon and Zagotta, 1995a), using 1 μM Ni^{2+} at a saturating concentration of the best agonist. Continuous curves represent fits of the dose-response relation to the Hill equation, $I = I_{max}([cNMP]^n/(K_{1/2}{}^n + [cNMP]^n))$. For fits to the activation of channels by cGMP (*C*), the following parameters were used: wt, $K_{1/2}$ = 79 μM, n = 2.1, I/I_{max} = 0.911; wt/wt, $K_{1/2}$ = 81 μM, n = 2, I/I_{max} = 0.889; D604M, $K_{1/2}$ = 251 μM, n = 1.5, I/I_{max} = 0.032; D604M/D604M, $K_{1/2}$ = 240 μM, n = 1.3, I/I_{max} = 0.026. For fits to the activation of channels by cAMP (*D*), the following parameters were used: wt, $K_{1/2}$ = 2334 μM, n = 1.5, I/I_{max} = 0.002; wt/wt, $K_{1/2}$ = 3061 μM, n = 1.3, I/I_{max} = 0.003; D604M, $K_{1/2}$ = 1629 μM, n = 1.2, I/I_{max} = 0.218; D604M/D604M, $K_{1/2}$ = 1136 μM, n = 1.2, I/I_{max} = 0.215.

Subunit interactions during the allosteric transition(s) associated with channel activation

The activation of CNG channels can be divided into two processes: ligand-binding steps and allosteric transitions leading to channel opening. "Allosteric" refers to a conformational change in the channel protein induced by the binding of ligand. There are at least two general classes of schemes that explain how the allosteric conformational changes associated with channel opening may occur in a multi-subunit channel where each subunit binds a single cyclic nucleotide (Fig. 2). One possibility is that the conformational transition(s) in the subunits that occur after binding of cyclic nucleotide may involve independent conformational changes in one, two, three, or four of the channel subunits (Fig. 2 *A*). Channel opening would take place after the requisite number of subunits underwent the appropriate independent conformational transition. In this case, the subunits are assumed to behave in an identical and independent manner. Alternatively, some cooperativity may occur between these transitions in the channel subunits. Cooperativity could arise from specific interactions between subunits during the allosteric transition(s), or from some special property of the open state, such as stabilization of

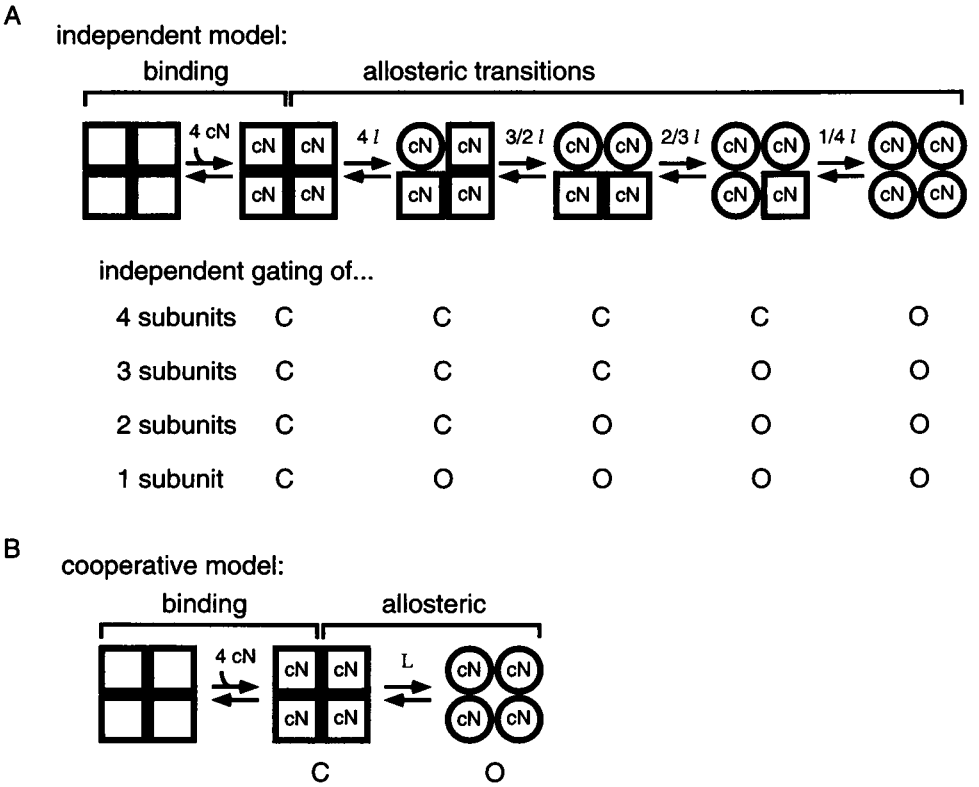

FIGURE 2 Schemes depicting general models for (*A*) independent and (*B*) cooperative allosteric transition(s) during CNG channel activation. Shown are events associated with channel activation that occur after initial binding of ligand, at saturating concentration of cyclic nucleotide (cN). C denotes closed channel conformations, and O indicates open channel conformations. Channel stoichiometry is assumed to be tetrameric.

the open channel due to hydration energy or ion occupancy in the pore. In the extreme case, a highly cooperative mechanism would behave as if there were a single concerted allosteric transition involving all of the subunits (Fig. 2 *B*). These models (Fig. 2, *A* and *B*) represent opposite extremes; other intermediate schemes are, of course, possible. For example, cooperative interactions could occur within subunit dimers, but each dimer could act independently. We will address the particular schemes outlined in Fig. 2 because they present reasonable hypotheses for CNG channel gating and they make distinct predictions about the behavior of channels containing different combinations of mutant and wild-type subunits. To examine these possibilities, we tested heteromultimeric channels generated by concatenated cDNA encoding dimers of wild-type and mutant subunits.

At saturating concentration of ligand, all of the binding sites are expected to be occupied, and the fractional activation (I_{sat}/I_{max}) reflects the ability of the agonist to promote the closed-to-open transition of the fully liganded channel. The current under these conditions (I_{sat}), normalized to the maximum current obtained after Ni^{2+} potentiation at saturating concentration of the best agonist (I_{max}), is a good measure of the equilibrium for the closed-to-open transition(s). Changes in I_{sat}/I_{max} for mutations and ligands examined in this paper most likely reflect a change in open probability rather than a change in single-channel conductance, because 1) the mutations are in the cyclic nucleotide binding domain and presumably distant from the channel pore, 2) it has been demonstrated previously that different cyclic nucleotides produce similar single-channel conductances (Ildefonse et al., 1992), and 3) after Ni^{2+} potentiation, currents produced by different cyclic nucleotides generally displayed a similar amplitude (data not shown). In Fig. 3 *A*, representative currents evoked at saturating cGMP by depolarizations to +60 mV from a holding potential of 0 mV are shown for wild-type (wt/wt) and mutant (D604M/D604M) homomultimers, and for wt/D604M and D604M/wt heteromultimers. These traces were normalized to I_{max} as described above. The heteromultimers were intermediate in agonist efficacy compared to wild-type and mutant homomultimers (Fig. 3 *A*). The similar behavior of the two heterodimers, where the mutant subunit is in either the N-terminal (D604M/wt) or C-terminal (wt/D604M) half of the dimer fusion protein, suggests that channel assembly occurred by association of two dimers rather than in some anomalous fashion, such as association of dimer halves (McCormack et al., 1992; Liman et al., 1992). If the channels formed preferentially from only the N-terminal half of the dimer, then we would expect the two different heterodimers to behave differently. Furthermore, this finding implies that the channel stoichiometry is some multiple of 2, and is consistent with a tetrameric quaternary structure for the functional channel complex (MacKinnon, 1991; Shen et al., 1994; MacKinnon, 1995). If the channel stoichiometry were not a multiple of 2, then expression of heterodimers would produce channels with unequal contributions from the respective dimer halves.

From I_{sat}/I_{max} we determined the apparent equilibrium constant (L_{app}) for the allosteric transition(s), treating the

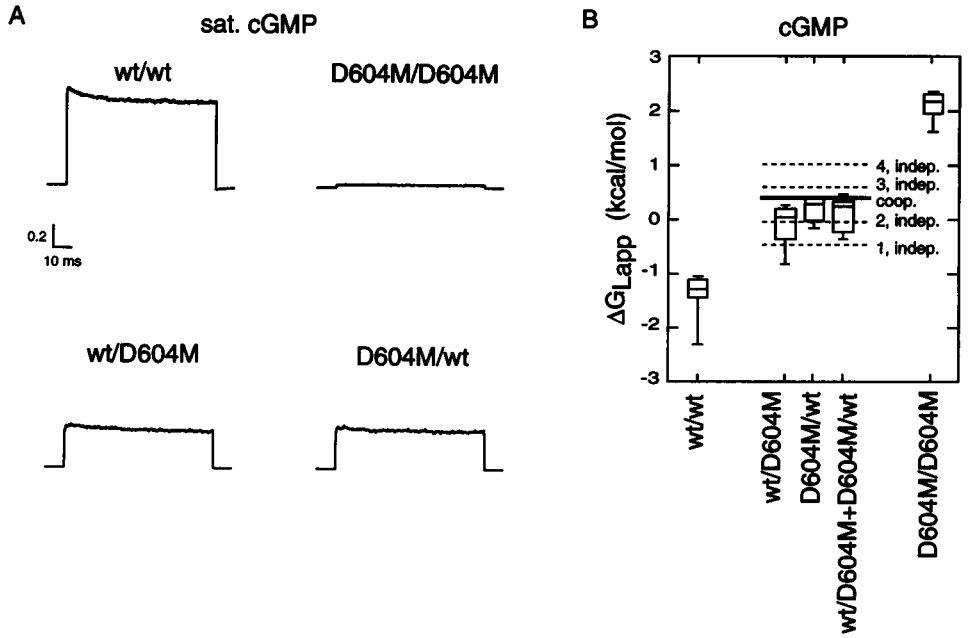

FIGURE 3 (*A*) Currents elicited by voltage steps from 0 mV to 60 mV are shown for activation of wt/wt and D604M/D604M homomultimeric channels and wt/D604M and D604M/wt heteromultimeric channels by saturating cGMP (8 mM). Vertical scale bars indicate fractional activation; currents were normalized to the maximum current (I_{max}) estimated from potentiation by 1 μM Ni^{2+} at a saturating concentration of the best agonist. (*B*) Box plot of the change in free energy for the aggregate equilibrium constant, $\Delta G_{L_{app}}$. The vertical line within each box indicates the median of the data; boxes show the 25th and 75th percentiles of the data; whiskers show the range of the data (N = 5 to 8). The expected free energy change for gating of the heteromultimeric channels, predicted by each of the different models for channel activation outlined in Fig. 2, is displayed as dashed (independent models) and solid (cooperative model) lines. These predictions were calculated using Eqs. 1 through 6 (see Materials and Methods).

ensemble of fully liganded closed and open states as a single closed-to-open transition, using the following equation:

$$L_{app} = (I_{sat}/I_{max})/[1 - (I_{sat}/I_{max})].$$

From the aggregate equilibrium constant L_{app}, we calculated the apparent change in free energy for the allosteric transition(s):

$$\Delta G_{L_{app}} = -RT \ln (L_{app}).$$

Fig. 3 *B* displays the effect of the D604M mutation on the $\Delta G_{L_{app}}$ for activation of CNG channels by cGMP. The free energy change of the apparent equilibrium constant for channel opening was approximately 3.5 kcal/mol less favorable for D604M/D604M mutant homodimers compared to wild-type homodimers. Expression of heterodimers containing the D604M mutation (wt/D604M or D604M/wt) gave median values for $\Delta G_{L_{app}}$ approximately halfway between those of the respective homomultimeric channels. Coexpression of the reciprocal heterodimers (wt/D604M + D604M/wt) yielded a $\Delta G_{L_{app}}$ similar to that observed for the individual heterodimers. These results suggest that the aspartic acid residue at position 604 in each subunit of a presumably tetrameric channel contributes approximately 0.9 kcal/mol to the allosteric conformational change(s) leading to channel opening.

Given the free energy change for the allosteric transitions of the wild-type and mutant homomultimers, we derived the expected free energy change for gating of the heteromultimeric channels predicted by each of the different models for the allosteric transition(s) outlined in Fig. 2. Each model was fit to the data for the wild-type and mutant homodimers, treating the allosteric transition(s) as a single aggregate closed-to-open transition. Then, using the parameters derived for each subunit (wild-type or mutant), we calculated the expected $\Delta G_{L_{app}}$ (using Eqs. 1–6, above) for heteromultimers containing two mutant and two wild-type subunits. In Fig. 3 *B*, these predictions are displayed as dashed (independent models) and solid (cooperative model) lines and compared to observed values for heteromultimeric channels. The $\Delta G_{L_{app}}$ for the activation of heteromultimeric channels (wt/D604M, D604M/wt, and wt/D604M + D604M/wt) by saturating cGMP was most consistent with a concerted transition to the open state (Fig. 3 *B*, *solid line*). Gating mechanisms that required separate and identical transitions in all four subunits or a single independent transition in only one of four subunits were largely incompatible with the observed values of $\Delta G_{L_{app}}$ for activation of these heteromultimeric channels. However, a mechanism involving an independent conformational change in any two subunits could also account for the behavior of heteromultimeric channels at saturating cGMP.

We also examined wild-type and D604M homodimers, and wt/D604M and D604M/wt heterodimers for activation by cIMP (Fig. 4 *A*). The structure of cIMP differs from that of cGMP only at the C2 position of the purine ring; it is a

good partial agonist for the rod CNG channel. As was the case for cGMP, agonist efficacy for currents evoked by saturating cIMP was reduced in D604M homodimers compared to wild-type homodimers. wt/D604M and D604M/wt heterodimers were intermediate in agonist efficacy compared to wild-type and mutant homodimers, and the reciprocal heterodimers behaved similarly. The D604M mutation made the apparent free energy change of the allosteric transition induced by cIMP less favorable by approximately 2.1 kcal/mol or about 0.5 kcal/mol per subunit (Fig. 4 *B*). Again, the ΔG_{Lapp} for the heteromultimeric channels was consistent with a concerted model for channel activation. These results were also compatible with a mechanism for the allosteric transition(s) involving an independent conformational change in two or three but not one or four of the channel subunits. Thus, results for cIMP were qualitatively similar to those presented in Fig. 3 for activation of D604M dimers by cGMP.

These conclusions were also consistent with the activation of these heteromultimeric channels by saturating concentrations of cAMP. In contrast to the effect on currents evoked by cGMP and cIMP, the D604M mutation improved agonist efficacy for currents evoked by cAMP (Fig. 5 *A*), making the free energy difference of the apparent equilibrium constant for the allosteric transition more favorable by approximately 1.9 kcal/mol for D604M/D604M mutant homodimers compared to wild-type homodimers (Fig. 5 *B*). As was observed above for cGMP and cIMP, I_{sat}/I_{max} for activation of wt/D604M and D604M/wt heterodimers by saturating cAMP was intermediate compared to wild-type and D604M/D604M homodimers (Fig. 5 *A*), and the ΔG_{Lapp} calculated for the activation of the heteromultimeric channels by cAMP was intermediate compared to ΔG_{Lapp} for the respective homomultimeric channels (Fig. 5 *B*). As demonstrated above, these results for cAMP were compatible with a concerted model for the allosteric transition or a model involving independent transitions in two or three of the subunits (Fig. 5 *B*).

We considered another mutation within the cyclic nucleotide binding domain of the channel, T560A, which primarily alters the affinity for cGMP and cAMP (Altenhofen et al., 1991) and has a smaller effect on the allosteric transition(s) (Varnum et al., 1995). T560A may be important for initial binding, presumably via contacts with the cyclic phosphate, and for positioning of the cyclic nucleotide for subsequent interactions during the conformational changes accompanying channel opening (Varnum et al., 1995). As can be seen in Fig. 6 *A*, the T560A mutation made ΔG_{Lapp} less favorable for activation of channels by cGMP. Activation of T560A homodimers by cIMP (Fig. 6 *B*) and cAMP (Fig. 6 *C*) demonstrated a slightly more favorable ΔG_{Lapp} compared to wild-type homodimers. As previously shown for D604M channels, expression of heteromultimeric channels composed of wild-type and T560A subunits demonstrated ΔG_{Lapp} values intermediate to those seen for the respective homomultimeric channels (Fig. 6). When compared with the ΔG_{Lapp} predicted by the various schemes, the results observed for activation of T560A heteromultimeric channels did not allow us to easily distinguish between the different models.

Coexpression of the reciprocal heterodimers (wt/T560A + T560A/wt) produced channels that behaved differently from the individual heterodimers. For activation of channels at saturating cGMP, the ΔG_{Lapp} was more like that of wild-type homomultimeric channels. For activation at saturating cIMP, the ΔG_{Lapp} resembled that of mutant homomultimeric channels. Assuming a random association of heterodimeric subunits and head-to-tail assembly, half of the presumably tetrameric channels from the coexpression would have a mutant subunit adjacent to a mutant subunit

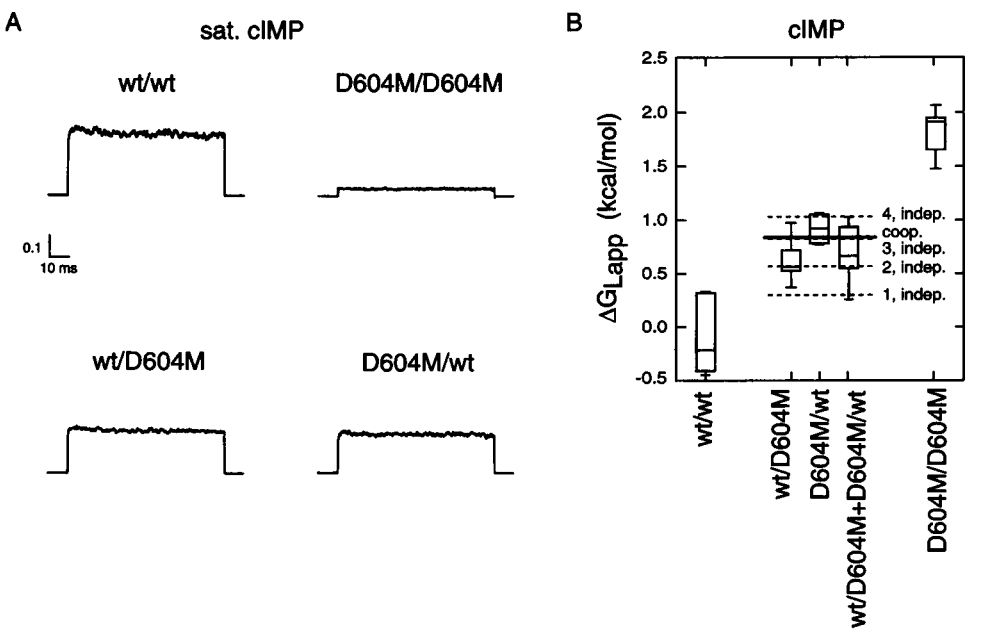

FIGURE 4 (*A*) Currents elicited by voltage steps from 0 mV to 60 mV are shown for activation of wt/wt and D604M/D604M homomultimeric channels and wt/D604M and D604M/wt heteromultimeric channels by saturating cIMP (32 mM). Vertical scale bars indicate fractional activation; currents were normalized to the maximum current (I_{max}) estimated from potentiation by 1 μM Ni^{2+} at saturating concentration of the best agonist. (*B*) Box plot of the change in free energy for the aggregate equilibrium constant, ΔG_{Lapp}, for activation by saturating cIMP. Values were calculated and displayed as described in Fig. 3 (N = 5 to 8).

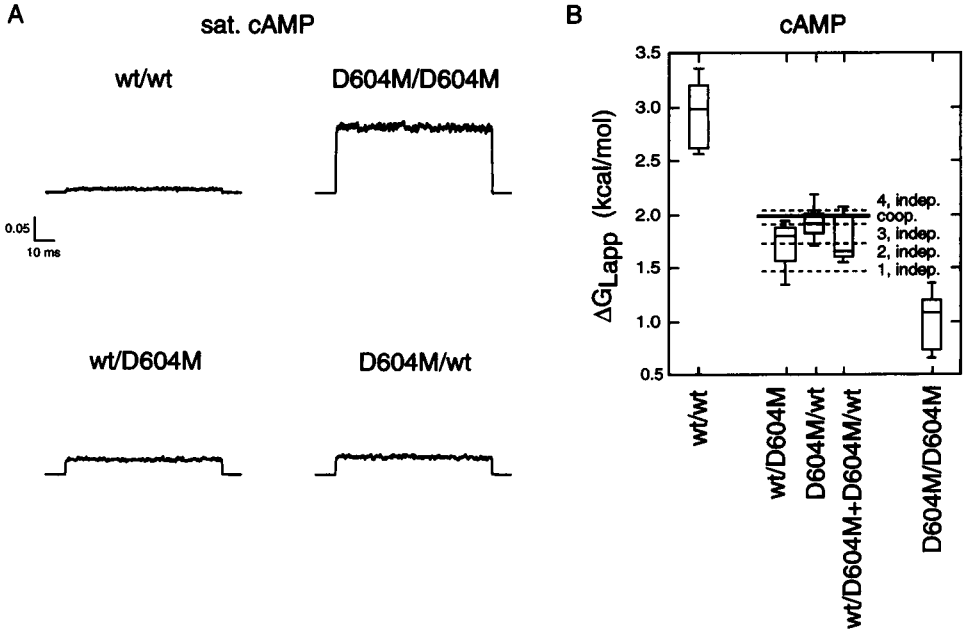

FIGURE 5 (*A*) Currents elicited by voltage steps from 0 mV to 60 mV are shown for activation of wt/wt and D604M/D604M homomultimeric channels and wt/D604M and D604M/wt heteromultimeric channels by saturating cAMP (32 mM). Vertical scale bars indicate fractional activation; currents were normalized to the maximum current (I_{max}) estimated from potentiation by 1 μM Ni^{2+} at saturating concentration of the best agonist. (*B*) Box plot of the change in free energy for the aggregate equilibrium constant, ΔG_{Lapp}, for activation by saturating cAMP. Values were calculated and displayed as described in Fig. 3 (N = 5 to 8).

and a wild-type subunit adjacent to a wild-type subunit, and the other half of the channel population would be assembled from identical dimers, alternating wild-type and mutant subunits (each subunit type diagonally opposed to its like subunit) (Gordon and Zagotta, 1995b). Activation of channels assembled from reciprocal heterodimers appeared to be influenced more by the "best" subunits when those subunits could be positioned adjacent to each other. These results suggest that the exact quaternary arrangement of mutant and wild-type subunits may be important for some mutations and that the subunits may not exhibit an equal and independent effect on channel gating.

Overall, the simplest interpretation of these results is that activation of CNG channels involves cooperative interactions between the channel subunits. However, it was not always possible to distinguish between different models, given the small effect on ΔG_{Lapp} for particular combinations of mutation and ligand. Where the range of values between wild-type and mutant was most marked, and thus the differences between the predictions of the models conspicuous (e.g., D604M, cGMP; Fig. 3 *B*), the results were inconsistent with a mechanism requiring separate and identical transitions in all of four subunits or a single independent transition in only one of four subunits. Although the results were consistent with cooperative interactions between subunits, the data were also compatible with schemes that include independent gating transitions in two or three of the channel subunits. Thus, we could not definitively discriminate between the appropriateness of a concerted model for CNG channel gating versus a model that envisions channel gating by independent transitions in two or three of the subunits.

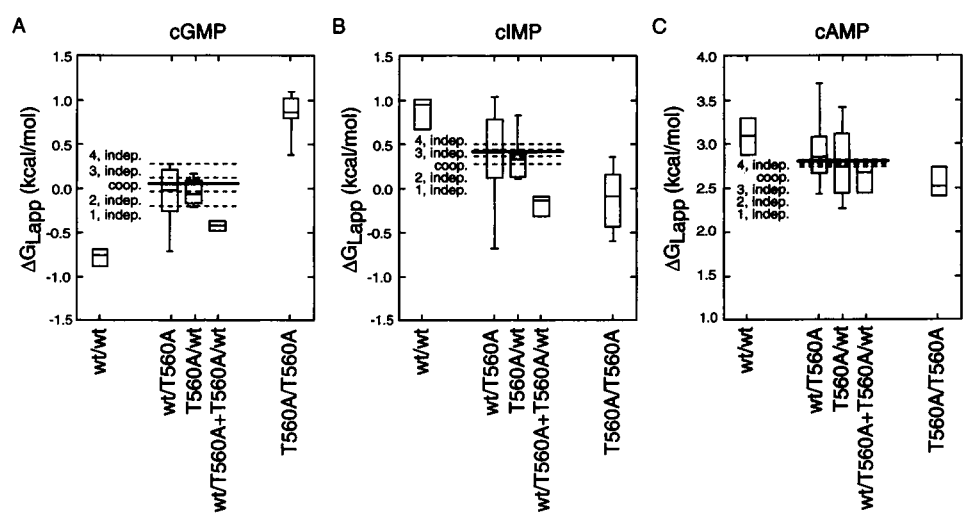

FIGURE 6 Box plot of the change in free energy for the aggregate equilibrium constant, ΔG_{Lapp}, for activation of wt/wt and T560A/T560A homomultimeric channels and wt/T560A and T560A/wt heteromultimeric channels by saturating cGMP (*A*; 16 mM), cIMP (*B*; 32 mM), and cAMP (*C*; 32 mM). Values were calculated and displayed as described in Fig. 3 (N = 4 to 8).

Monod, Wyman, and Changeux model for activation of heteromultimeric channels

In the previous section, we investigated subunit interactions during the allosteric transition(s) using saturating concentrations of ligand. To consider events associated with ligand binding, we have also examined activation of heteromultimeric CNG channels at subsaturating ligand concentrations (Fig. 7). As expected, the apparent affinity of the heteromultimeric channels (wt/D604M and D604M/wt) was intermediate to that of the respective homomultimeric channels (wt/wt and D604M/D604M) for activation by cGMP (Fig. 7 *A*), cIMP (Fig. 7 *B*), and cAMP (Fig. 7 *C*). The slopes of the dose-response curves were similar, consistent with a single population of channels. Furthermore, the reciprocal heterodimers (wt/D604M and D604M/wt) displayed similar apparent affinities, again suggesting that channel assembly occurred by association of two dimers, and consistent with a tetrameric structure for the CNG channel.

Because our results at saturating concentration of cyclic nucleotide were consistent with a concerted mechanism for CNG channel activation, we next examined a specific gating scheme that includes a concerted conformational transition to the open state, the allosteric model of Monod, Wyman, and Changeux (Monod et al., 1965). The MWC model was first proposed to describe the activation of CNG channels of retinal photoreceptors by Stryer (1987). Recently, a MWC model for CNG channel activation has been shown to be consistent with the steady-state characteristics of cloned bovine rod and catfish olfactory channels (Goulding et al., 1994). In a MWC-type scheme, the channel is proposed to exist in two reversibly accessible quaternary states: a tense or closed state (C), and a relaxed or open state (O). Assuming a tetrameric structure for the channel and that each subunit of the channel binds a single cyclic nucleotide, then four equivalent binding sites are present. This model can be summarized by the following scheme:

Scheme 1

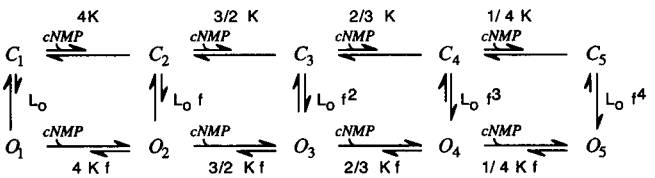

In the closed configuration, the cyclic nucleotide binds to each subunit with a bimolecular equilibrium constant K. The affinity of the binding sites for ligand is altered when the transition between the two conformations occurs, the affinity for the open state being greater than the affinity for the closed state. Conversely, the conformational transition between the closed and open states is promoted by binding of ligand to each site. The factor by which the equilibrium constant for opening is increased by each ligand binding step is designated as f.

Unlike other possible concerted models for channel activation, the concerted opening conformational change in the MWC model does not absolutely require ligand binding but is favored by binding of ligand to each subunit. Interestingly, two groups have recently reported evidence for ligand-independent opening of CNG ion channels (Picones and Korenbrot, 1995; Tibbs et al., 1995), consistent with one of the fundamental predictions of a MWC model. The equilibrium constant for the conformational transition between the unliganded form of C and the unliganded form of O is defined as L_O. At saturating concentrations of ligand,

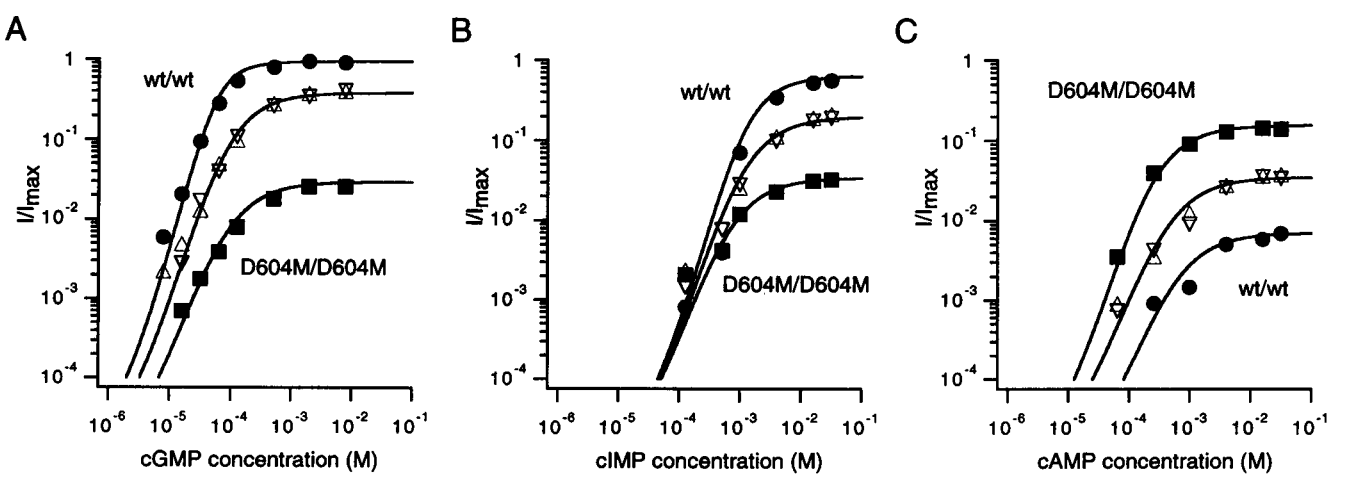

FIGURE 7 Dose-response relations for activation of wt/wt (●) and D604M/D604M (■) homomultimeric channels and wt/D604M (△) and D604M/wt (▽) heteromultimeric channels by cGMP (*A*), cIMP (*B*), and cAMP (*C*). Continuous curves show fits of the MWC scheme to the dose-response relationship using the following parameters: in all cases, $L_O = 1.4 \times 10^{-5}$; for activation of wild-type subunits by cGMP, $f = 30.7$ and $K = 12000\ M^{-1}$; for activation of D604M subunits by cGMP, $f = 6.8$ and $K = 20000\ M^{-1}$; for activation of wild-type subunits by cIMP, $f = 18.7$ and $K = 900\ M^{-1}$; for activation of D604M subunits by cIMP, $f = 7.1$ and $K = 2500\ M^{-1}$; for activation of wild-type subunits by cAMP, $f = 4.7$ and $K = 2800\ M^{-1}$; for activation of D604M subunits by cAMP, $f = 10.7$ and $K = 6200\ M^{-1}$.

all four binding sites are assumed to be occupied, and the channel is in either the fully liganded open or fully liganded closed state; the equilibrium constant for this allosteric transition is $f^4 \cdot L_O$ and can be determined as follows:

$$f^4 \cdot L_O = (I_{sat}/I_{max})/[1 - (I_{sat}/I_{max})].$$

The only free parameters in the MWC scheme are f, L_O, and K. Mutations or conditions that modify channel activation can be modeled to alter one or more of these three parameters. For example, potentiation of CNG channels by Ni^{2+} (Gordon and Zagotta, 1995a) probably has a general affect on L_O, promoting the allosteric conformational transition in a manner relatively independent of ligand type or concentration. In contrast, for D604M channels the effect of the mutation on the allosteric transition is profoundly dependent on the nature of the ligand (Varnum et al., 1995), suggesting that this mutation alters f with little or no effect on L_O. For T560A channels, the functional consequences of the mutation for initial binding affinity, and to a lesser extent for the allosteric transition, imply an effect on K and f rather than L_O. In general, mutation or modification of residues outside the cyclic nucleotide binding pocket that affect the allosteric transition(s) would be expected to alter L_O. Mutation of residues that directly interact with the cyclic nucleotide during the allosteric transition would be expected to affect f. Thus, we assumed that L_O was not altered by D604M or T560A, and only f and K were allowed to vary for MWC fits to dose-response data for channels containing these mutations. A small alteration in L_O cannot be completely excluded.

In a heteromultimeric channel, the subunits do not behave identically, and thus the simplified MWC scheme shown above must be extended to account for the nonequivalency of the subunits. In Fig. 8, the tense or closed channel subunits are depicted as squares and the relaxed or open channel subunits are depicted as circles. Mutant subunits are denoted by an M, and ligand occupancy of a subunit is indicated by shading. From every state shown there can be a concerted allosteric transition between the closed and open channel configurations. The equilibrium constant for the allosteric transition will depend on which of the subunits, wild-type or mutant (M), are occupied by ligand.

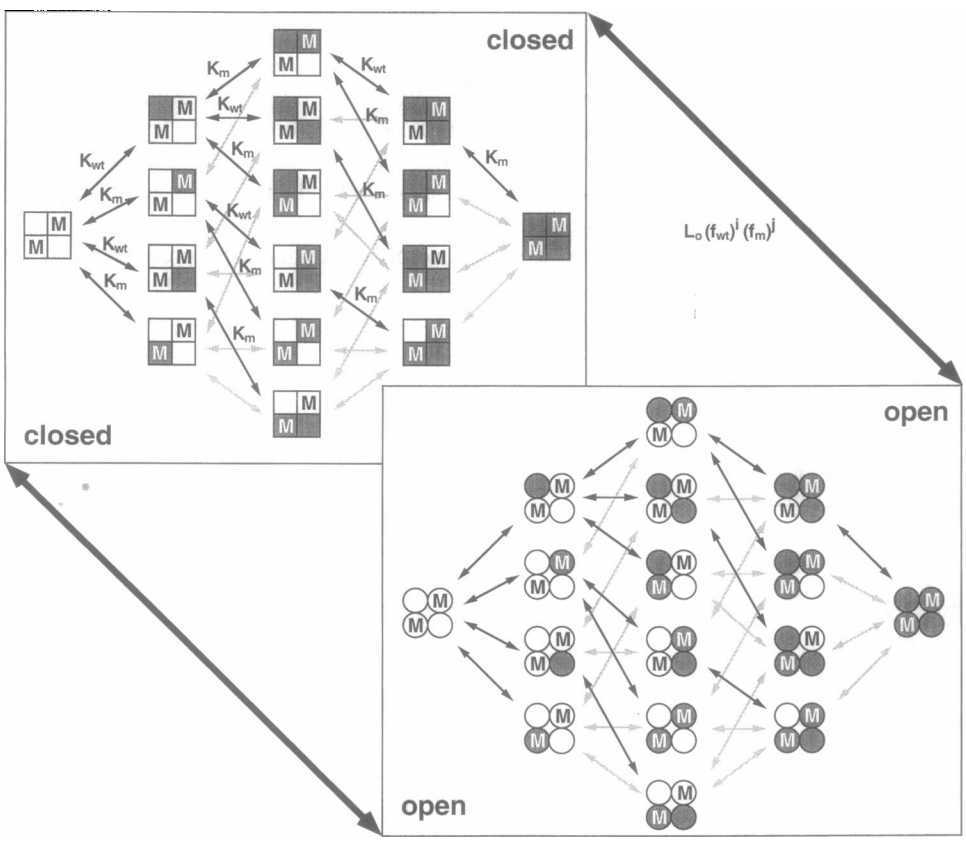

FIGURE 8 Monod, Wyman, and Changeux scheme for activation of heteromultimeric CNG channels. Channels are proposed to exist in one of two possible quaternary conformations. Closed or tense channel subunits are indicated by squares; open or relaxed channel subunits are indicated by circles. M denotes mutant subunits; shading depicts ligand occupancy. For transitions involving ligand binding, a single pathway to every state is indicated by dark arrows. K_{wt} and K_m are the bimolecular equilibrium constants for ligand binding to wild-type and mutant subunits, respectively. The concerted allosteric transition between the closed- and open-channel configurations can occur from any of the states shown. Transitions between the open and closed states have an equilibrium constant equal to $L_O(f_{wt})^i(f_m)^j$, where i is equal to the number of wild-type subunits with bound cNMP, j is the number of mutant subunits with bound cNMP, f_{wt} and f_m are the factors by which the equilibrium constant for opening is increased by ligand binding to wild-type and mutant subunits, respectively, and L_O is the equilibrium constant for the conformational transition between the unliganded closed state and the unliganded open state.

This scheme was used to fit the data for the heteromultimeric channels using the L_O, f, and K values derived from fits of data from homomultimeric channels. As can be seen in Fig. 7, the MWC model provided a reasonable fit to the dose-response data for activation of wild-type and D604M homomultimeric channels and heteromultimeric channels comprised of both types of subunits. An L_O equivalent for bovine rod channels has been suggested from the literature, 1×10^{-6} (Stryer, 1987) or 1×10^{-5} (Goulding et al., 1994). For our fits, L_O was estimated to be 1.4×10^{-5} and was not permitted to vary. The effect of the D604M mutation on f was dependent on which particular cyclic nucleotide was used to activate the channels: f became less favorable for activation of channels by cGMP (Fig. 7 *A*) and cIMP (Fig. 7 *B*), but more favorable for activation of channels by cAMP (Fig. 7 *C*). For cGMP, f was approximately 30.7 for wild-type subunits and 6.8 for mutant subunits; for cIMP, f was approximately 18.7 and 7.1, respectively; for cAMP, f was approximately 4.7 and 10.7, respectively. In the context of the MWC model, these results are consistent with the proposed role for this residue in ligand discrimination and in conveying ligand binding to the allosteric changes associated with channel opening (Varnum et al., 1995). For all cyclic nucleotides tested, K became slightly more favorable when the number of D604M subunits increased. For the D604M mutation, the free energy change for initial binding became more favorable by approximately 0.3 kcal/mol for cGMP, 0.6 kcal/mol for cIMP, and 0.5 kcal/mol for cAMP. Replacement of aspartic acid by methionine at this position may directly or indirectly facilitate ligand binding, perhaps by removing an electrostatic or steric hindrance for access to the ligand-binding pocket.

For T560A-containing channels, the most profound effect of the mutation is on initial cGMP affinity (Altenhofen et al., 1991; Varnum et al., 1995). Consequently, dose-response curves for activation of T560A homomultimeric and heteromultimeric channels by cGMP offered a better test for a MWC model of CNG channel gating than D604M channels. The MWC model provided a reasonable fit to the dose-response data for activation of T560A channels by cGMP (Fig. 9 *A*). Again, L_O was held constant at 1.4×10^{-5}, and only K and f were permitted to vary. For this model, a large effect of the T560A mutation on K was observed for activation of these channels by cGMP. The free energy change for initial binding of cGMP became approximately 1.2 kcal/mol less favorable for T560A. The effect on f was less pronounced for T560A subunits (approximately 27.0 for wild-type versus 11.6 for mutant subunits). Fits of the MWC model were also consistent with activation of these channels by cIMP (Fig. 9 *B*) and cAMP (Fig. 9 *C*).

DISCUSSION

In this paper, we have examined possible subunit interactions during the activation of homomultimeric and heteromultimeric CNG channels. At saturating concentrations of ligand, the effect on ΔG_{Lapp} of introducing D604M or T560A mutations in the ligand-binding domain of half of the channel subunits was consistent with a concerted model for the allosteric transition. Results were also consistent with a model involving independent conformational transitions in two or three of the subunits. Models for channel activation that involve independent transitions in all four channel subunits or a single independent transition in only one of the subunits could not account for the data. In addition, steady-state dose-response relations for activation

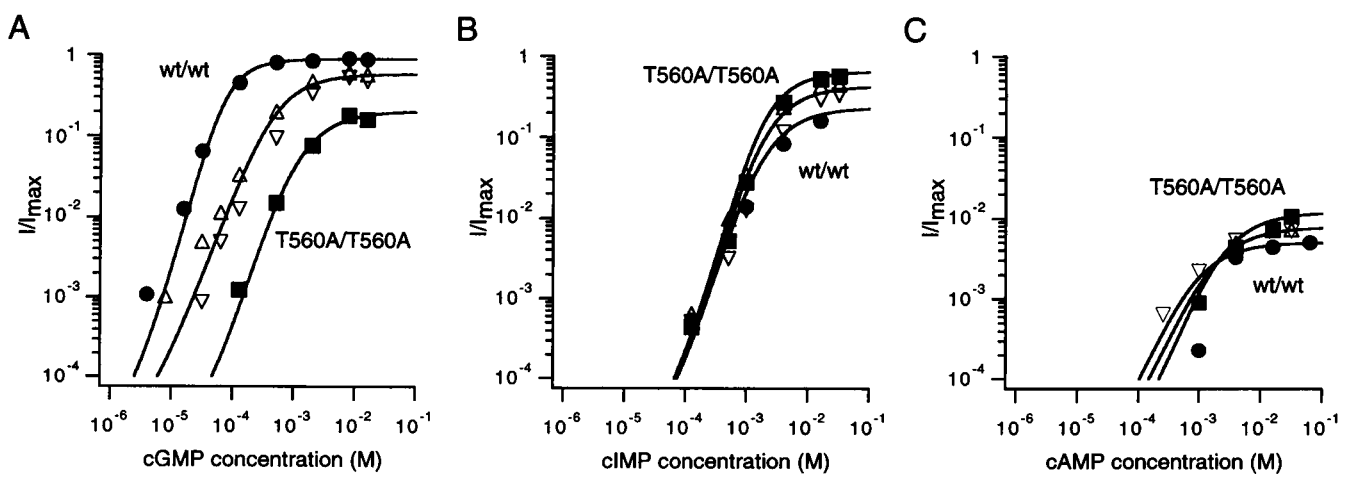

FIGURE 9 Dose-response relations for activation of wt/wt (●) and T560A/T560A (■) homomultimeric channels and wt/T560A (△) and T560A/wt (▽) heteromultimeric channels by cGMP (*A*), cIMP (*B*), and cAMP (*C*). Continuous curves show fits of the MWC scheme to the dose-response relationship using the following parameters: in all cases, $L_O = 1.4 \times 10^{-5}$; for activation of wild-type subunits by cGMP, $f = 27$ and $K = 11000\ M^{-1}$; for activation of T560A subunits by cGMP, $f = 11.6$ and $K = 1500\ M^{-1}$; for activation of wild-type subunits by cIMP, $f = 12.1$ and $K = 900\ M^{-1}$; for activation of T560A subunits by cIMP, $f = 19.1$ and $K = 600\ M^{-1}$; for activation of wild-type subunits by cAMP, $f = 4.4$ and $K = 2000\ M^{-1}$; for activation of T560A subunits by cAMP, $f = 5.4$ and $K = 850\ M^{-1}$.

of heteromultimeric channels were found to be consistent with a MWC model involving a single concerted allosteric transition promoted by binding of ligand to the channel subunits.

In these experiments, the similar behavior of the reciprocal heterodimers was consistent with a tetrameric quaternary structure for the functional CNG channel complex. In photoreceptors and olfactory neurons, channels probably exist as heteromultimers of at least two types of subunits (Chen et al., 1993, 1994; Korschen et al., 1995; Liman and Buck, 1994; Bradley et al., 1994). One function of the recently identified second subunits may be to tune the sensitivity of the channels to cGMP and cAMP in these cell types (Bradley et al., 1994; Liman and Buck, 1994). Results presented in this paper, from expression of heteromultimeric channels with aspartic acid at position 604 replaced with methionine (as is present in the rat olfactory second subunit) in half of the channel subunits, are consistent with this possible role. This result demonstrates that the D604M difference in the second subunit of the olfactory channel can account for the increase in cAMP sensitivity, even if it is not present in all of the channel subunits.

The dose-response data for the heteromultimers helps to exclude other models for CNG channel activation. Because fits of the Hill equation to the dose-response data often yield Hill coefficients near 2, it might be expected that maximum activation of CNG channels would be produced by binding of cyclic nucleotide to only two subunits. If binding of cyclic nucleotide to any two subunits was sufficient for maximum channel activation, then heterodimers would be predicted to display affinities that more closely resembled wild-type homomultimers, a prediction that is not supported by the data. A variation of this scheme requires binding of ligand to any two adjacent subunits. This provides a better fit to the dose-response data for the individual heteromultimers. This scheme predicts that channels assembled from coexpressed heterodimers should activate better than the individual heterodimers, as observed for the T560A heterodimers (Fig. 6, *A* and *B*). However, this effect for coexpressed heterodimers was not as apparent for D604M heterodimers (Figs. 3 *B*, 4 *B*, and 5 *B*).

The functional symmetry of the CNG channel at the level of the binding domain is not known. A twofold symmetry has been suggested for proton binding in the channel pore (Root and MacKinnon, 1994) and for Ni^{2+} binding near the inner vestibule of the pore (Gordon and Zagotta, 1995b). We have assumed that the channel oligomer displays fourfold symmetry at the level of the binding domain and that the position of each binding domain is essentially equivalent. However, one possibility is that the channel's four cyclic nucleotide binding domains interact as two functional pairs (Goulding et al., 1994). The interaction between the binding domains within each pair could present either positive or negative cooperativity. In support of this notion is the finding that coexpression of the reciprocal T560A heterodimers produced channels that differed somewhat from those produced by expression of the individual heterodimers. One way in which the position of the subunits may matter is if the cyclic nucleotide-binding sites are structurally overlapping, as is the case for a homologous protein–the catabolite gene activator protein (CAP). The crystal structure of the CAP dimer indicates that the purine ring of bound cAMP is stabilized in part by hydrogen bonds with T127 of the C α-helix of one subunit and with S128 of the contralateral subunit (Weber and Steitz, 1987). Sequence comparisons between the cyclic nucleotide-binding domain of CNG channels and CAP suggest that amino acid D604 of the rod channel aligns with this region of CAP (T127). The structural analogy with CAP is consistent with the possibility that these domains may dimerize and that D604 may be directly or indirectly involved in intersubunit interactions.

We thank Kevin D. Black, Gay Sheridan, and Lorie Devlin for expert technical assistance; and Richard W. Aldrich, Sharona E. Gordon, and Mark S. Shapiro for comments on the manuscript. In addition, we thank E. R. Liman for the high expression vector.

This work was supported by a grant from the National Eye Institute (EY 10329 to WNZ and the Human Frontier Science Program). WNZ is an Investigator and MDV is an Associate of the Howard Hughes Medical Institute.

REFERENCES

Altenhofen, W., J. Ludwig, E. Eismann, W. Kraus, W. Bonigk, and U. B. Kaupp. 1991. Control of ligand specificity in cyclic nucleotide-gated channels from rod photoreceptors and olfactory epithelium. *Proc. Natl. Acad. Sci. USA.* 88:9868–9872.

Biel, M., X. Zong, M. Distler, E. Bosse, N. Klugbauer, M. Murakami, V. Flockerzi, and F. Hofmann. 1994. Another member of the cyclic nucleotide-gated channel family, expressed in testis, kidney, and heart. *Proc. Natl. Acad. Sci. USA.* 91:3505–3509.

Bradley, J., J. Li, N. Davidson, H. A. Lester, and K. Zinn. 1994. Heteromeric olfactory cyclic nucleotide-gated channels: a subunit that confers increased sensitivity to cAMP. *Proc. Natl. Acad. Sci. USA.* 91: 8890–8894.

Chen, T. Y., M. Illing, L. L. Molday, Y. T. Hsu, K. W. Yau, and R. S. Molday. 1994. Subunit 2 (or beta) of retinal rod cGMP-gated cation channel is a component of the 240-kDa channel-associated protein and mediates Ca(2+)-calmodulin modulation. *Proc. Natl. Acad. Sci. USA.* 91:11757–11761.

Chen, T. Y., Y. W. Peng, R. S. Dhallan, B. Ahamed, R. R. Reed, and K. W. Yau. 1993. A new subunit of the cyclic nucleotide-gated cation channel in retinal rods. *Nature.* 362:764–767.

Dhallan, R. S., K. W. Yau, K. A. Schrader, and R. R. Reed. 1990. Primary structure and functional expression of a cyclic nucleotide-activated channel from olfactory neurons. *Nature.* 347:184–187.

Distler, M., M. Biel, V. Flockerzi, and F. Hofmann. 1994. Expression of cyclic nucleotide-gated cation channels in non-sensory tissues and cells. *Neuropharmacology.* 33:1275–1282.

Dryer, S. E., and D. Henderson. 1991. A cyclic GMP-activated channel in dissociated cells of the chick pineal gland. *Nature.* 353:756–758.

Gordon, S. E., and W. N. Zagotta. 1995a. A histidine residue associated with the gate of the cyclic nucleotide-activated channels in rod photoreceptors. *Neuron.* 14:177–183.

Gordon, S. E., and W. N. Zagotta. 1995b. Subunit interactions in coordination of Ni^{2+} in cyclic nucleotide-gated channels. *Proc. Natl. Acad. Sci. USA.* 92:10222–10226.

Goulding, E. H., J. Ngai, R. H. Kramer, S. Colicos, R. Axel, S. A. Siegelbaum, and A. Chess. 1992. Molecular cloning and single-channel properties of the cyclic nucleotide-gated channel from catfish olfactory neurons. *Neuron.* 8:45–58.

Goulding, E. H., G. R. Tibbs, and S. A. Siegelbaum. 1994. Molecular mechanism of cyclic-nucleotide-gated channel activation. *Nature.* 372: 369–374.

Heginbotham, L., and R. MacKinnon. 1992. The aromatic binding site for tetraethylammonium ion on potassium channels. *Neuron.* 8:483–491.

Hurst, R. S., M. P. Kavanaugh, J. Yakel, J. P. Adelman, and R. A. North. 1992. Cooperative interactions amoung subunits of a voltage-dependent potassium channel. *J. Biol. Chem.* 267:23742–23745.

Ildefonse, M., S. Crouzy, and N. Bennett. 1992. Gating of retinal rod cation channel by different nucleotides: comparative study of unitary currents. *J. Membr. Biol.* 130:91–104.

Jan, L. Y., and Y. N. Jan. 1990. A superfamily of ion channels. *Nature.* 345:672.

Kaupp, U. B., and K. W. Koch. 1992. Role of cGMP and Ca^{2+} in vertebrate photoreceptor excitation and adaptation. *Annu. Rev. Physiol.* 54:153–175.

Kaupp, U. B., T. Niidome, T. Tanabe, S. Terada, W. Bonigk, W. Stuhmer, N. J. Cook, K. Kangawa, H. Matsuo, T. Hirose, T. Miyata, and S. Numa. 1989. Primary structure and functional expression from complementary DNA of the rod photoreceptor cyclic GMP-gated channel. *Nature.* 342:762–766.

Kavanaugh, M. P., R. S. Hurst, J. Yakel, M. D. Varnum, J. P. Adelman, and R. A. North. 1992. Multiple subunits of a voltage-dependent potassium channel contribute to the binding site for tetraethylammonium. *Neuron.* 8:493–497.

Korschen, H. G., M. Illing, R. Selfert, F. Sesti, A. Williams, S. Gotzes, C. Colville, F. Muller, A. Dose, M. Godde, L. Molday, U. B. Kaupp, and R. S. Molday. 1995. A 240 kDa protein represents the complete β subunit of the cyclic nucleotide-gated channel from rod photoreceptor. *Neuron.* 15:627–636.

Lancet, D. 1986. Vertebrate olfactory reception. *Annu. Rev. Neurosci.* 9:329–355.

Liman, E. R., and L. B. Buck. 1994. A second subunit of the olfactory cyclic nucleotide-gated channel confers high sensitivity to cAMP. *Neuron.* 13:611–621.

Liman, E. R., J. Tytgat, and P. Hess. 1992. Subunit stoichiometry of a mammalian K^+ channel determined by construction of multimeric cDNAs. *Neuron.* 9:861–871.

MacKinnon, R. 1991. Determination of the subunit stoichiometry of a voltage-activated potassium channel. *Nature.* 350:232–235.

MacKinnon, R. 1995. Pore loops: an emerging theme in ion channel structure. *Neuron.* 14:889–892.

McCormack, K., L. Lin, L. Iverson, M. Tanouye, and F. Sigworth. 1992. Tandem linkage of Shaker K^+ channel subunits does not ensure the stoichiometry of expressed channels. *Biophys. J.* 63:1406–1411.

Monod, J., J. Wyman, and J. P. Changeux. 1965. On the nature of allosteric transitions: a plausible model. *J. Mol. Biol.* 12:88–118.

Ogielska, E. M., W. N. Zagotta, T. Hoshi, S. Heinemann, J. Haab, and R. W. Aldrich. 1995. Cooperative subunit interactions in C-type inactivation of K channels. *Biophys. J.* 69:2449–2457.

Picones, A., and J. I. Korenbrot. 1995. Spontaneous, ligand-independent activity of the cGMP-gated ion channels in cone photorecptors of fish. *J. Physiol. (Lond.).* 485:699–714.

Root, M. J., and R. MacKinnon. 1994. Two identical noninteracting sites in an ion channel revealed by proton transfer. *Science.* 265:1852–1856.

Shabb, J. B., and J. D. Corbin. 1992. Cyclic nucleotide-binding domains in proteins having diverse functions. *J. Biol. Chem.* 267:5723–5726.

Shen, K.-Z., A. Lagrutta, N. W. Davies, N. B. Standen, J. P. Adelman, and R. A. North. 1994. Tetraethylammonium block of Slowpoke calcium-activated potassium channels expressed in *Xenopus* oocytes: evidence for tetrameric channel formation. *Pflugers Arch.* 426:440–445.

Stryer, L. 1987. Visual transduction: design and recurring motifs. *Chemica Scripta.* 27B:161–171.

Su, Y., W. R. G. Dostmann, F. W. Herberg, K. Durick, N.-h. Xuong, L. Ten Eyck, S. S. Taylor, and K. I. Varughese. 1995. Regulatory subunit of protein kinase A: structure of deletion mutant with cAMP binding domains. *Science.* 269:807–813.

Tibbs, G. R., E. H. Goulding, and S. A. Siegelbaum. 1995. Spontaneous opening of cyclic nucleotide-gated channels supports and allosteric model of activation. *Biophys. J.* 68:A253.

Tytgat, J., and P. Hess. 1992. Evidence for cooperative interactions in potassium channel gating. *Nature.* 359:420–423.

Varnum, M. D., K. D. Black, and W. N. Zagotta. 1995. Molecular mechanism for ligand discrimination of cyclic nucleotide-gated channels. *Neuron.* 15:619–625.

Weber, I. T., and T. A. Steitz. 1987. Structure of a complex of catabolite gene activator protein and cyclic AMP refined at 2.5 Å resolution. *J. Mol. Biol.* 198:311–326.

Weyand, I., M. Godde, S. Frings, J. Weiner, F. Muller, W. Altenhofen, H. Hatt, and U. B. Kaupp. 1994. Cloning and functional expression of a cyclic-nucleotide-gated channel from mammalian sperm. *Nature.* 368: 859–863.

Yau, K. W., and D. A. Baylor. 1989. Cyclic GMP-activated conductance of retinal photoreceptor cells. *Annu. Rev. Neurosci.* 12:289–327.

Zagotta, W. N., T. Hoshi, and R. W. Aldrich. 1989. Gating of single Shaker potassium channels in Drosophila muscle and in *Xenopus* oocytes injected with Shaker mRNA. *Proc. Natl. Acad. Sci. USA.* 86:7243–7247.

Zimmerman, A. L., J. W. Karpen, and D. A. Baylor. 1988. Hindered diffusion in excised membrane patches from retinal rod outer segments. *Biophys J.* 54:351–355.

Zufall, F., S. Firestein, and G. M. Shepherd. 1994. Cyclic nucleotide-gated ion channels and sensory transduction in olfactory receptor neurons. *Annu. Rev. Biophys. Biomol. Struct.* 23:577–607.